

# Confocal Raman thermometer for microfluidic devices

Guillermo D. Brinatti Vazquez<sup>a,b</sup>, Oscar E. Martínez<sup>a,b</sup> and Juan Martín Cabaleiro<sup>a,c,d</sup>

<sup>a</sup> Consejo Nacional de Investigaciones Científicas y Técnicas, Argentina.

<sup>b</sup> Laboratorio de Fotónica, Facultad de Ingeniería, Universidad de Buenos Aires, Argentina.

<sup>c</sup> Laboratorio de Fluidodinámica, Facultad de Ingeniería, Universidad de Buenos Aires, Argentina.

<sup>d</sup> Laboratorio de Micro y Nanofluídica y Plasma, UdeMM, Buenos Aires, Argentina.

## ABSTRACT

A confocal Raman microscopy technique has been designed and demonstrated that measures the temperature rise and profile in microfluidic devices. The system is based in the deformation of the water Raman peak assigned to the O-H stretching at  $3400\text{ cm}^{-1}$  that occurs with temperature keeping an isosbestic point at  $3425\text{ cm}^{-1}$ . Hence two photon counting detectors that sample the Raman emission at each side of the isosbestic point are used to monitor the water temperature. Using a confocal detection scheme the spatial resolution of a confocal microscope can be obtained to map the temperature profile within small microfluidic structure in a noninvasive manner. The differential signal between the two channels normalized by the added signals has a linear dependence with temperature that yields a sensitivity of  $0.8\text{ K}$  using a  $1\text{ s}$  integration time and a count rate per channel of  $1.5 \cdot 10^5$ . The pump laser used had a  $405\text{ nm}$  wavelength and  $20\text{ mW}$  average power. The confocal collection was performed by a single mode optical fiber and the explored volume was of about  $40\text{ }\mu\text{m}^3$ . The temperature rise in electrofluidic devices was studied showing that the temperature increase depended on the power used to move the sample along the channel (electroosmotic flow) and the particular design and structure of the device that determines the heat dissipation mechanism. The scheme proved useful to evaluate and prevent detrimental temperature effects with the advantage that no specific temperature sensitive particle needs to be added to the fluid, and has the additional virtue of allowing spatial scans in 3D.

**Keywords:** Microfluidic devices, Joule Heating, Temperature, Raman thermometer

## 1. INTRODUCTION

Electroosmotic pumping and electrophoresis are the main strategies to move liquid or species in microfluidic devices.<sup>1,2</sup> In any of the latter, an electric current is passed through the liquid, resulting in Joule heat dissipation on the medium. This will cause a temperature rise on the device that will depend on its dissipation efficiency. As these techniques are often used in biological applications<sup>3</sup> an undesired temperature rise could change drastically the experiment evolution or even make it fail. Also, as the electroosmotic and electrophoretic mobility are a function of temperature<sup>4</sup> a poor thermal control could lead to an unexpected pumping behavior. This is why temperature monitoring and dissipation efficiency characterization are of great importance in the field. The readers are referred to the reviews by Xuan<sup>5</sup> and Cetin and Li<sup>6</sup> for a deeper description of joule heating in electrokinetic flows.

With this purpose different techniques were introduced to measure temperature inside microchannels. A common approach is to make use of thermal properties in fluorescent dyes to indirectly measure temperature from fluorescence imaging.<sup>4,7-10</sup> This involves introducing an additional compound in the flow that could modify chemical reactions occurring inside the microchannel, making the method unsuitable for online monitoring. Moreover, the measurement “integrates” the temperature in the channel height, not allowing for the measurement of temperature profiles normal to the channel bottom.

---

Further author information: (Send correspondence to G. D. Brinatti Vazquez)

G. D. Brinatti Vazquez: E-mail: guillermobrinatti@gmail.com, Telephone: +54 11 5285 0828

O. E. Martínez: E-mail: omartinez@fi.uba.ar, Telephone: +54 11 5285 0828

J. M. Cabaleiro: Email: jmcabaleiro@gmail.com, Telephone: +54 11 5285 0467

Walrafen et al<sup>11</sup> discovered that the infrared spectrum of water shows temperature dependent qualities and measured the existence of an isosbestic point around  $3425\text{ cm}^{-1}$ . This molecular property can be sensed using Raman Scattering to get a temperature dependent signal that is intrinsic of water. This method was proposed and proved useful in microchannels<sup>12-14</sup> where an epi-illumination microscope was adapted to measure the Raman spectrum by exciting the water with a visible laser. Temperature is then recovered by analyzing these spectra. As water absorption is low in visible wavelengths<sup>15</sup> this method proved to be non-invasive.

In this work we propose a device which improves from previous attempts by improving spatial resolution using a confocal collection scheme and by increasing the acquisition speed by splitting the spectrum in the isosbestic point and sending each portion to an independent detector. This results in a device capable of mapping temperature in three dimensions, allowing to study the thermal properties of the flow and the different surfaces of the microfluidic device. Also, a correlation between the temperature profile and the type of flow is shown. Additionally, a dark field illumination scheme is used to collect scattering or fluorescence images of the sample at the same time temperature measurements take place.

## 2. EXPERIMENT

The device proposed to measure the temperature inside microfluidic devices is depicted in figure 1. A 150 mW laser diode emitting at 405 nm is used as excitation beam. The light is coupled to a single mode (SM) optical fiber (using aspheric lenses L0 and L1) acting as spatial filter. The light exiting the fiber is collimated by a triplet lens (L2) and sent into the microscope by reflecting in a long pass dichroic mirror (420 LP) centered in 420 nm. A short pass filter (450 SP) is used to block any light in the detection band. The light then reflects in a second long pass dichroic mirror (505 LP) centered in 505 nm and then is focused in the sample using a 40X 0.95 NA microscope objective. The total power in the sample at 405 nm is around 25 mW.

The Raman scattering (around 470 nm) collected by the same objective is separated from the excitation path as it is transmitted in the first dichroic mirror. The light is then coupled to a Multi mode (MM) optical fiber (10  $\mu\text{m}$  core diameter) using a 10X 0.28 NA microscope objective. This step gives the microscope confocal resolution as the light coming from outside the confocal volume will have a poor coupling efficiency. The other end of the optical fiber is sent to a light tight enclosure containing the detection part of the setup, where the light is collimated and directed to a 300 lines/mm diffraction grating (DG). An achromatic lens is used to focus the diffracted light into a D shaped mirror (DM) mounted in a translation stage used to split the spectrum at the isosbestic point. Each new light path is then directed to a independent photon counter (PMT A and PMT B) for detection. A lens (LA and LB) and a longpass filter (FA and FB) are used before the detector to get an image of the plane of DM and to remove light at the laser wavelength. The voltage pulses coming from the detectors are registered by a on board, two channel, 32 bit counter in a PC.

The sample is also illuminated in a dark field scheme using a 10 mW laser beam emitting at 520 nm. The scattering or fluorescence produced by this beam is then separated from the pump and signal beam as it is transmitted trough 505 LP. A 100 mm tube lens is used to get a image of the sample on a CMOS camera. This is used to set the sample in place and to track particles incorporated in the liquid in order to measure flow velocity. This can be used to study the flow inside the microchannel without interfering with the signal path if low particle concentrations are used to avoid fluorescence signals excited by the pump beam that could lay in the Raman spectrum. As the confocal volume is small, the probability of such event is also small if low concentrations are used.

As the collection is confocal a three dimensional characterization of the sample is possible with the proper scanning mechanism. In this application we choose to use a three axis motorized stage to move the sample in all dimensions. A galvo mirror design is also possible in applications where speed is required. Two angular degrees of freedom are used in the sample holder in order to set the detection plane parallel to the microchannels. The axial resolution achieved with the setup is of 9  $\mu\text{m}$  resulting in a collection volume of around 40  $\mu\text{m}^3$  with a photon count rate of  $1.5 \cdot 10^5\text{ s}^{-1}$  on each detector.

Microfluidics chips were made by polydimethylsiloxane (PDMS) replication of a Silicon-SU8 master. The PDMS microchannels produced were sealed with 150  $\mu\text{m}$  thick glass coverslips. To improve the superficial bond between glass and PDMS, both parts were exposed to microwave air plasma and then gently held together. The

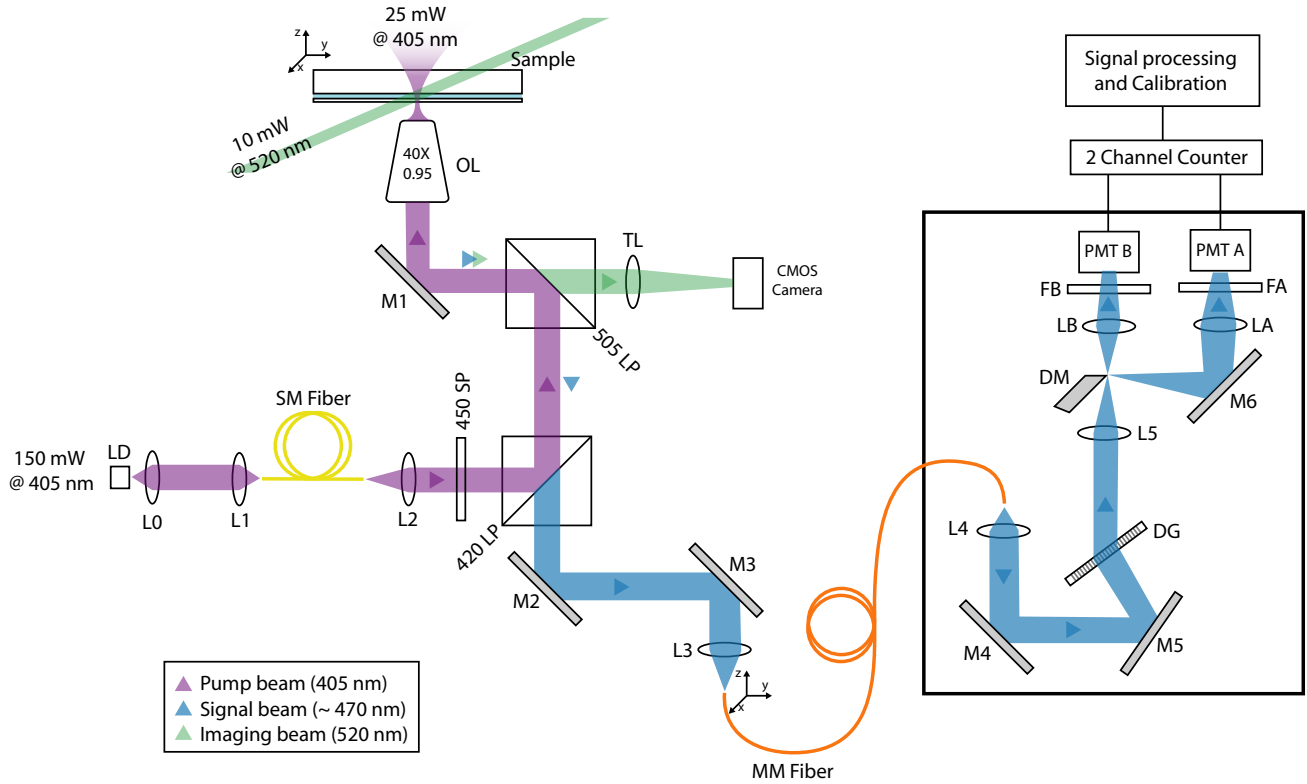


Figure 1. Schematic representation of the microscope used for Raman thermometry. A 150 mW laser diode emitting in 405 nm (LD) is used as excitation beam. A single mode (SM) fiber is used as a spatial filter before focusing the beam on the sample using a 40X 0.95 NA microscope objective. A dichroic mirror centered in 420 nm is used to separate the collected Raman emission (centered around 470 nm) which is focused in a Multi mode (MM) fiber which grants confocal resolution. The output of the fiber is sent to a specially made spectroemeter which split the spectrum at the isosbestic point and sent each channel to a independent photon counter device. Signal processing and calibration is made in a PC. A 10 mW, 520 nm beam is used to illuminate the sample in a dark field scheme. This results in a scattering image of the sample in a CMOS camera.

plasma step is not mandatory due to the low manometric pressure into the channel, however plasma bonding allows for easier manipulation of the chip as the bonding is permanent. Plastic round reservoirs (made by cutting 10 ml plastic syringes, Diameter  $\sim 16$  mm) were attached to both ends of the straight microchannels. The channels were filled with a 5000  $\mu\text{S}/\text{cm}$  KCl solution. Polystyrene microspheres 1  $\mu\text{m}$  in diameter were incorporated to the fluid in a low concentration in order to set the proper initial condition (zero fluid velocity) before the electric field is turned on. This was achieved by detecting the scattering of the particles on the camera and tracking their positions. A power supply delivering up to 1 kV is used to establish the flow.

### 3. RESULTS AND DISCUSSION

First we start by showing a calibration for the technique in figure 2. This was made by using a temperature controlled water cell in the sample plane. By measuring simultaneously the temperature of the cell and the water using Raman thermometry we obtain a linear calibration. The spread of the data points around the linear fit result in a resolution of 0.8 K using a integration time of 1 s. All the measurements in this article were performed with this integration time.

The temperature rise at the center of each microchannel was measured using the technique as a function of the Joule heat dissipated in the device. The result of this experiment is shown in figure 3 where temperature rise is plotted against dissipated power per unit glass area for different channel geometries. A linear fit is displayed for each data set. For the three channels with 80  $\mu\text{m}$  height we can see that the slope of the linear feat is fairly

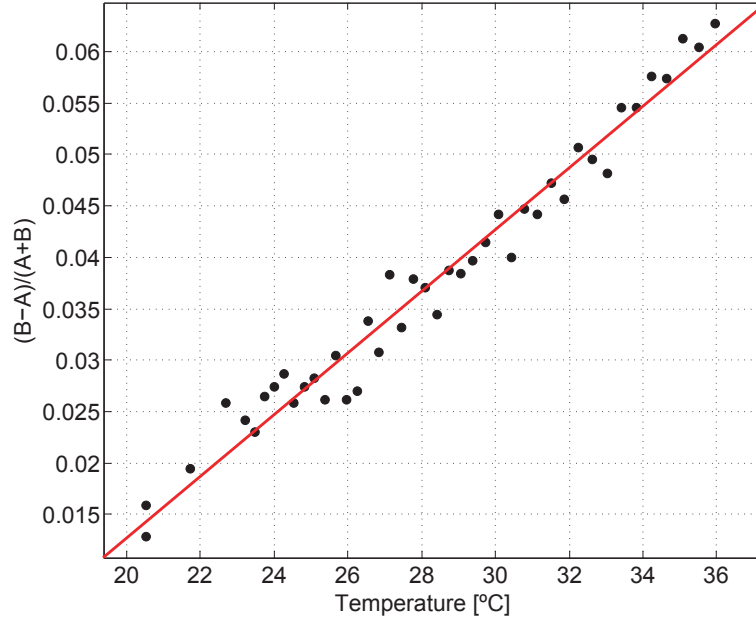


Figure 2. Temperature dependent signal as a function of temperature. A linear fit of the data results in a proper calibration. A resolution of 0.8 K is achieved with a 1 s integration time.

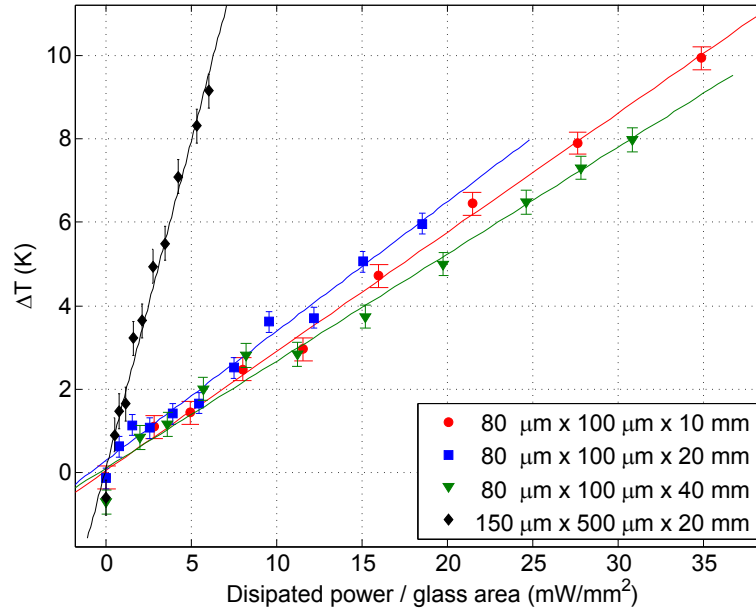


Figure 3. Temperature rise versus dissipated power per glass area for microchannels of different geometry. A linear fit is shown for each data set.

similar. This indicates that the glass floor of the device is the main dissipation mechanism, independently of the length of the channel. For the taller 150  $\mu\text{m}$  channel we see a drastic change in its slope, indicating a different heat flow in the channel.

As the technique is confocal 3D spatial scans are possible. In figure 4 a vertical scan from the center of the channel to the glass surface is shown. The same experiment was repeated for the smaller channels resulting in a constant temperature profile, in good agreement with theory and previous experiments. In the case of the wider channel, two different temperatures are observed separated by an abrupt change. The center of the channel about 3 K hotter than the water surrounding the base of the channel.

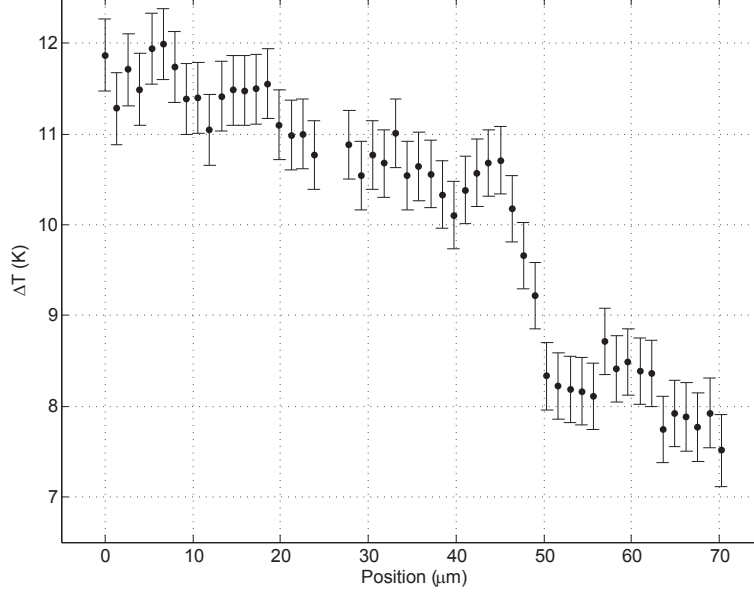


Figure 4. Temperature as a function of height from the center (left side) to the glass floor of the channel (right side) with dimensions  $150\text{ }\mu\text{m} \times 500\text{ }\mu\text{m} \times 20\text{ mm}$  (height x base x lenght).

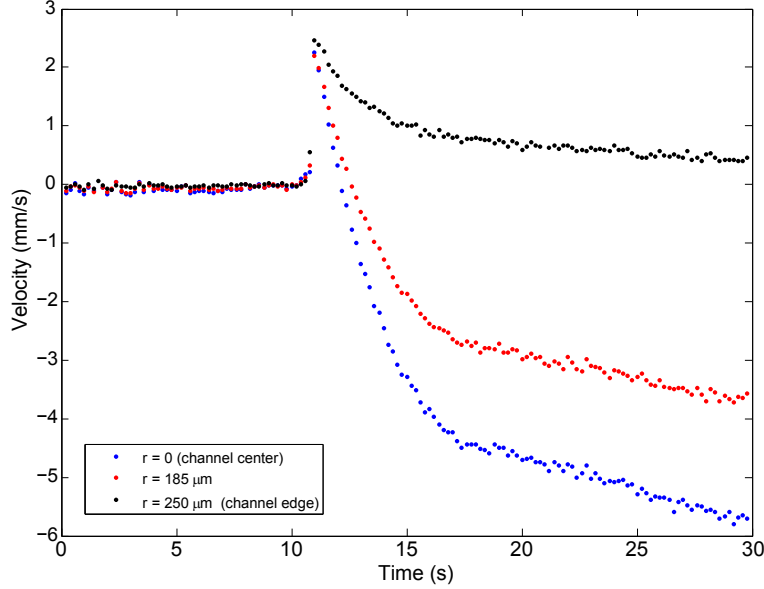


Figure 5. PIV measurement for the  $150\text{ }\mu\text{m} \times 500\text{ }\mu\text{m} \times 20\text{ mm}$  microchannel for three different positions form the center to the edge of the device.

For a complete characterization of the channels a Particle Imaging Velocimetry (PIV) measurement was independently performed in the same conditions for each device. Figure 5 shows the results of this experiment for the channel exhibiting a different behavior. The PIV corresponding to the small channels show a constant *plug type* flow in all the measuring interval. For this channel a an initial planar flow is observed when electric field is turned on around  $t = 11\text{ s}$ , but is rapidly lost due to the pressure difference generated between the reservoirs. This results in a parabolic flow in the opposite direction to the initial flow with a maximum at the center of the channel. With this information, results shown in figure 4 can be understood as the flow is bidirectional. The temperature jump between the two counterpropagating flows indicates the presence of a contact thermal impedance indicating that each stream is flowing without exchanging mass with its counterpart.

## 4. CONCLUSIONS

A novel technique to measure temperature in microfluidic devices is shown. The method uses the dependency on temperature of the Raman spectrum of water and improves from previous implementations that the collection is confocal, giving a improved three dimensional resolution, and the detection is made using a pair of photon counters which improves measuring time as is not necessary to measure the whole spectrum in each position. The technique shows good agreement with results from other methods and theoretical calculations.<sup>8</sup> We also show that the device is useful to characterize microfluidic chips, giving useful information for the election of dimensions and construction materials in the design stage.

The technique also shows a thermal behavior never reported before when a bidirectional flow is observed. Each flow develop its own temperature and a sharp gradient is observed at the interface. This was correlated with PIV measurements performed independently in the same conditions.

## REFERENCES

- [1] Hunter, R. J., [*Foundations of Colloid Science*], Oxford University Press, 2nd ed. (2001).
- [2] Lyklema, J. J., de Keizer, A., Bijsterbosch, B., Fleer, G., and (Eds.), M. C. S., [*Solid-Liquid Interfaces*], vol. 2 of *Fundamentals of Interface and Colloid Science*, Elsevier, Academic Press (1995).
- [3] Tian, W.-C. and Finehout, E., [*Microfluidics for Biological Applications*], Springer Publishing Company, Incorporated, 1 ed. (2008).
- [4] Tang, G., Yan, D., Yang, C., Gong, H., Chai, J. C., and Lam, Y. C., "Assessment of joule heating and its effects on electroosmotic flow and electrophoretic transport of solutes in microfluidic channels," *ELECTROPHORESIS* **27**(3), 628–639 (2006).
- [5] Xuan, X., "Joule heating in electrokinetic flow," *ELECTROPHORESIS* **29**(1), 33–43 (2008).
- [6] Cetin, B. and Li, D., "Effect of joule heating on electrokinetic transport," *ELECTROPHORESIS* **29**(5), 994–1005 (2008).
- [7] Ross, D., Gaitan, M., and Locascio, L. E., "Temperature measurement in microfluidic systems using a temperature-dependent fluorescent dye," *Analytical Chemistry* **73**(17), 4117–4123 (2001). PMID: 11569800.
- [8] Erickson, D., Sinton, D., and Li, D., "Joule heating and heat transfer in poly(dimethylsiloxane) microfluidic systems," *Lab Chip* **3**, 141–149 (2003).
- [9] Hsieh, S.-S. and Yang, T.-K., "Electroosmotic flow in rectangular microchannels with joule heating effects," *Journal of Micromechanics and Microengineering* **18**(2), 025025 (2008).
- [10] Fu, L.-M., Wang, J.-H., Luo, W.-B., and Lin, C.-H., "Experimental and numerical investigation into the joule heating effect for electrokinetically driven microfluidic chips utilizing total internal reflection fluorescence microscopy," *Microfluidics and nanofluidics* **6**(4), 499–507 (2009).
- [11] Walrafen, G., Fisher, M., Hokmabadi, M., and Yang, W.-H., "Temperature dependence of the low-and high-frequency raman scattering from liquid water," *The Journal of chemical physics* **85**(12), 6970–6982 (1986).
- [12] Davis, K. L., Liu, K. L. K., Lanan, M., and Morris, M. D., "Spatially resolved temperature measurements in electrophoresis capillaries by raman thermometry," *Analytical chemistry* **65**(3), 293–298 (1993).
- [13] Liu, K.-L. K., Davis, K. L., and Morris, M. D., "Raman spectroscopic measurement of spatial and temporal temperature gradients in operating electrophoresis capillaries," *Analytical chemistry* **66**(21), 3744–3750 (1994).
- [14] Kim, S. H., Noh, J., Jeon, M. K., Kim, K. W., Lee, L. P., and Woo, S. I., "Micro-raman thermometry for measuring the temperature distribution inside the microchannel of a polymerase chain reaction chip," *Journal of Micromechanics and Microengineering* **16**(3), 526 (2006).
- [15] Pegau, W. S., Gray, D., and Zaneveld, J. R. V., "Absorption and attenuation of visible and near-infrared light in water: dependence on temperature and salinity," *Applied optics* **36**(24), 6035–6046 (1997).